Proceedings of the 25th International Conference on
Port and Ocean Engineering under Arctic Conditions
June 9-13, 2019, Delft, The Netherlands

Long term prediction of local ice loads on the hull of S.A. Agulhas II

Pentti Kujala[1], Zongyu Jiang[1], Fang Li[1], Liangliang Lu[1]
[1]Department of Mechanical Engineering, Aalto University, Espoo, Finland

ABSTRACT

S.A. Agulhas II was instrumented in Finland in 2012 to measure full scale ice-induced loads on the hull. After the ship was delivered to South Africa, she has visited Antarctic every year. The level ice thickness is obtained from the visual observations during voyages of S.A. Agulhas II to the Antarctic. The local ice loads on hull was measured by the strain gauges mounted on frames at the bow, bow shoulder and stern shoulder. The long-term full scale database of S.A. Agulhas II has been established since the summer in 2012-2013 and our analysis is based on seven-year measurements (2012/13 to 2018/19). A statistical model is applied to predict the long term ice load on the hull of S.A. Agulhas II. In this model, the long term ice load is evaluated by using the peak values during a specific time period, which means the method focuses on the statistics of extreme value. This method establishes a connection between the ice loads and the prevailing ice conditions by using the measured mean and standard deviation of ice thickness and considering the ice thickness distribution following the normal probability distribution. The ice load measurements are used as benchmark to validate long term prediction provided by the statistical model.

KEY WORDS: Ice load; long-term prediction; Full scale measurement.

1. Introduction

A vessel is under impact of ice loads when she is operating in ice-covered waters. The ice loads can increase the resistance, undermine the stability and even damage the hull when it is sufficiently high. Therefore, it is meaningful to understand the characteristics of ice loads, especially the relationship between the ice loads and ice conditions.

Researchers have developed many approaches to study ice loads, such as full scale measurement, model scale test in ice tank and numerical simulation. Among these methods, the full scale measurement is the most reliable so far because the properties of sea ice is complicated and the ice breaking process is not fully comprehended (Kujala et al., 2019). The most interesting parameter of the full scale measurement is the extreme value of ice loads because it directly relates to the damage of hull. The extreme value of ice loads is stochastic according to the full scale measurement (Kujala et al., 2009; Chai et al., 2018). Consequently,

many probability distributions have been applied to predict the extreme ice loads, such as Exponential Gamma and Weibull distribution (Kujala et al., 2009), and Average Conditional Exceedance Rate (Chai et al., 2018).

Based on the comprehensive records from full scale and experimental tests, Kujala (1989ab, 1996) presents a semi-empirical approach to predict long term ice loads. This approach first statistically analyzes the ice induced loads on hull and ice conditions. By using this statistical analysis, a relationship is obtained between the ice loads and the prevailing ice conditions.

This paper firstly introduces the full scale measurement on board of a polar supply and research vessel S.A. Agulhas II. Secondly, the observed prevailing ice condition and extreme values of ice loads are presented in section 2 and 3. The Gumbel I asymptotic distribution is used to compare with the measurement. Thirdly, Kujala's method is utilized to predict the long term ice loads based on the connection between the ice loads and prevailing ice condition. This long term prediction is verified by five years' measurements onboard S.A. Agulhas II. Kujala's method proposes a statistic model to reflect the relationship between the ice thickness and ice loads. By using this model, the long term ice loads on ship can be predicted with known specific ice condition.

2. Full scale measurement on S.A. Agulhas II

Starting from 2012, S.A. Agulhas II voyages to the Antarctic every summer, commonly from December to next year's February. The common route starts from Cape Town, passes by Bouvet Island and arrives at the Akta Bukta/Neumayer III (the German Antarctic research station) and the SANAE IV (the South African Antarctic research station). The whole voyage also includes the route between the Neumayer III and South Georgia & the South Sandwich Islands, as shown in Figure 1. Therefore, S.A. Agulhas II encounters the ice loads in the waters shown in Figure 1. Unfortunately, the ice condition and ice area are complicated and vary every year so it is impossible to simply show the ice area in Figure 1. In addition, the purpose of this research is to discover the statistic relationship between the ice thickness and the ice loads but not to study the reason of change of ice thickness. Therefore, the exact ice area is not important to this research and consequently the ice area is not shown in Figure 1.

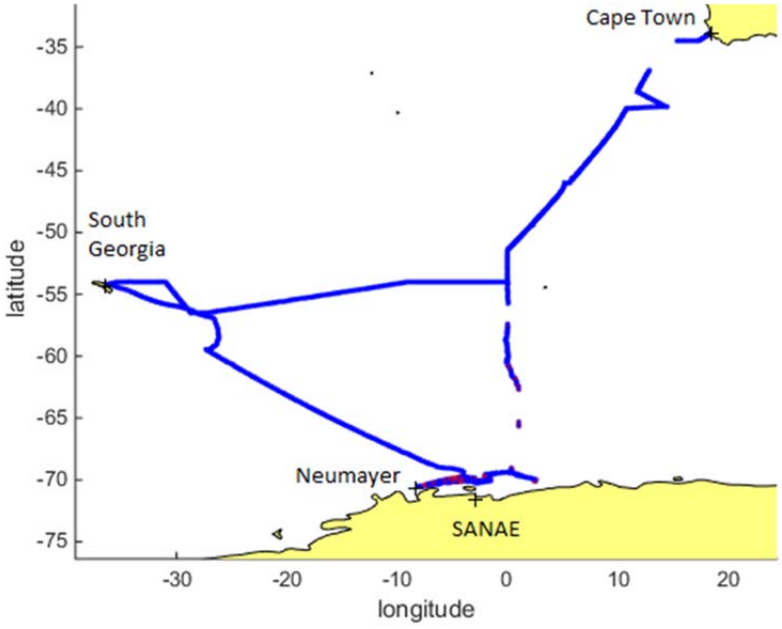

Figure 1. Common voyaging waters

2.1 S.A. Agulhas II and instrumentation

S.A. Agulhas II was designed and built as a Polar Supply and Research Vessel (PSRV). She was delivered in April 2012 with the Polar ice class PC 5 and the strength of the hull is constructed in accordance with DNV ICE-10. This enables her to navigate through the Antarctic waters. Table 1 presents the main dimensions of S.A. Agulhas II.

Table 1. The main dimensions of S.A. Agulhas II

Item	Value
Length, bpp. [m]	121.8
Breadth, mould. [m]	21.7
Draught, design [m]	7.65
Deadweight at design displacement [t]	5 000
Service speed [kn]	14.0

A measuring system was installed on board of S.A. Agulhas II in order to enhance the understanding of ice loads on the hull and propulsion system. The measuring system consists of ice condition observing instruments, ice loads measuring instruments, shaft line measuring instruments and whole-body vibration measuring instruments. Herein, only the instruments for ice condition observation and ice loads measurement are briefly described because they are related to the research content of this paper. For more details, the readers can refer to Suominen et al. (2013) and Bekker et al. (2014).

During the voyage, the ice conditions were recorded by visual observations. The observations were summarized for every ten-minute interval. The record consists of ice concentration, ice floe diameters and ice thicknesses. The ice thickness was recorded by observing ice blocks turned up by the ship hull for each minute. In addition, a stereo camera system, mounted at the bow shoulder, was also deployed to measure the ice thickness. The stereo camera system includes two industrial cameras which were separately connected to a computer via Ethernet links. These two cameras periodically take images of underneath ice blocks turned up by the hull. Thus, the information of ice thickness can be obtained by transferring the pixel unit thickness of image into millimeter unit.

The ice loads on the hull were measured with V-shape strain gauges. The strain gauges were permanently mounted on nine frames of the hull: two frames at the bow area, three frames at the bow shoulder area and four frames at the stern shoulder area. Figure 2 shows that two strain gauges were mounted on each frame. When a frame is deformed by sea ice, the upper and lower gauges measured different strains. The loads on the frame were calculated with the difference of strain measured by the two gauges. The calculation also considered the influence of neighbor frames (Bekker et al, 2014; Suominen et al., 2017).

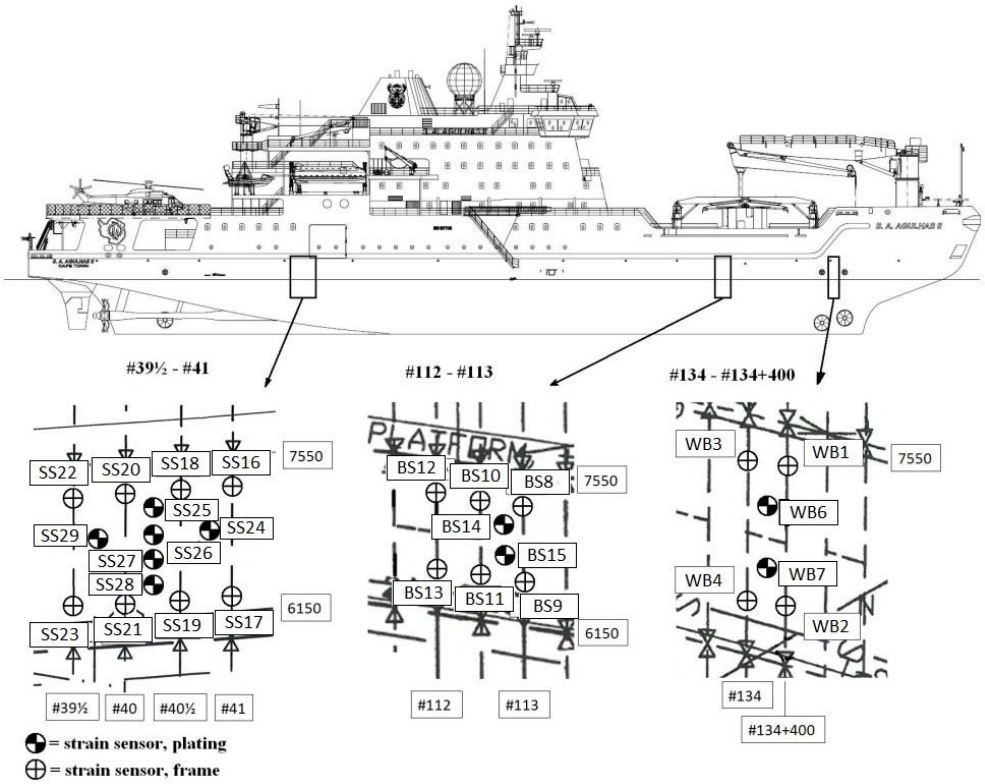

Figure 2. The strain gauge instrumentation on the hull

2.2 Ice condition

Researchers have developed various approaches to evaluate the thickness of sea ice, such as visual observation, sounding devices, electromagnetic device, and stereo camera systems. Among of them, the visual observation is a traditional method. Nevertheless, it shows good precision even though this method can be interrupted by many factors (Suominen et al, 2016). The ice thickness data in this paper is obtained by the visual observation. The visual observation can record many parameters of sea ice but only the ice thickness is discussed herein, since it is the most relevant parameter to evaluate the loads induced by the sea ice (Kujala et al, 2019).

Table 2. Parameter of ice thickness distribution

Parameter	2012 - 2013	2013 - 2014	2014 - 2015	2015 - 2016	2016 - 2017	2017 - 2018	2018 - 2019
Total number	576	2158	1466	1131	661	165	962
Mean [m]	0.9	1.4	0.6	0.8	0.7	0.7	0.5
Standard deviation [m]	0.5	0.6	0.5	0.5	0.4	0.3	0.3

Figure 3 shows the distribution of sea ice thickness recorded during the voyage of S.A. Agulhas II from 2012 to 2019. The time interval of observation is ten minutes. It is clearly indicated that the distribution of ice thickness varies year by year. The total number of recorded ice thickness varies intensely. Normally, the number of ice thickness is equal to the occurrence of ice contact, which is an important parameter in the calculation of return period. Therefore, this parameter influences the prediction of ice loads. The number, mean value and standard deviation of ice thickness are shown in Table 2. The mean value and standard

deviation of the ice thickness also varies intensely.

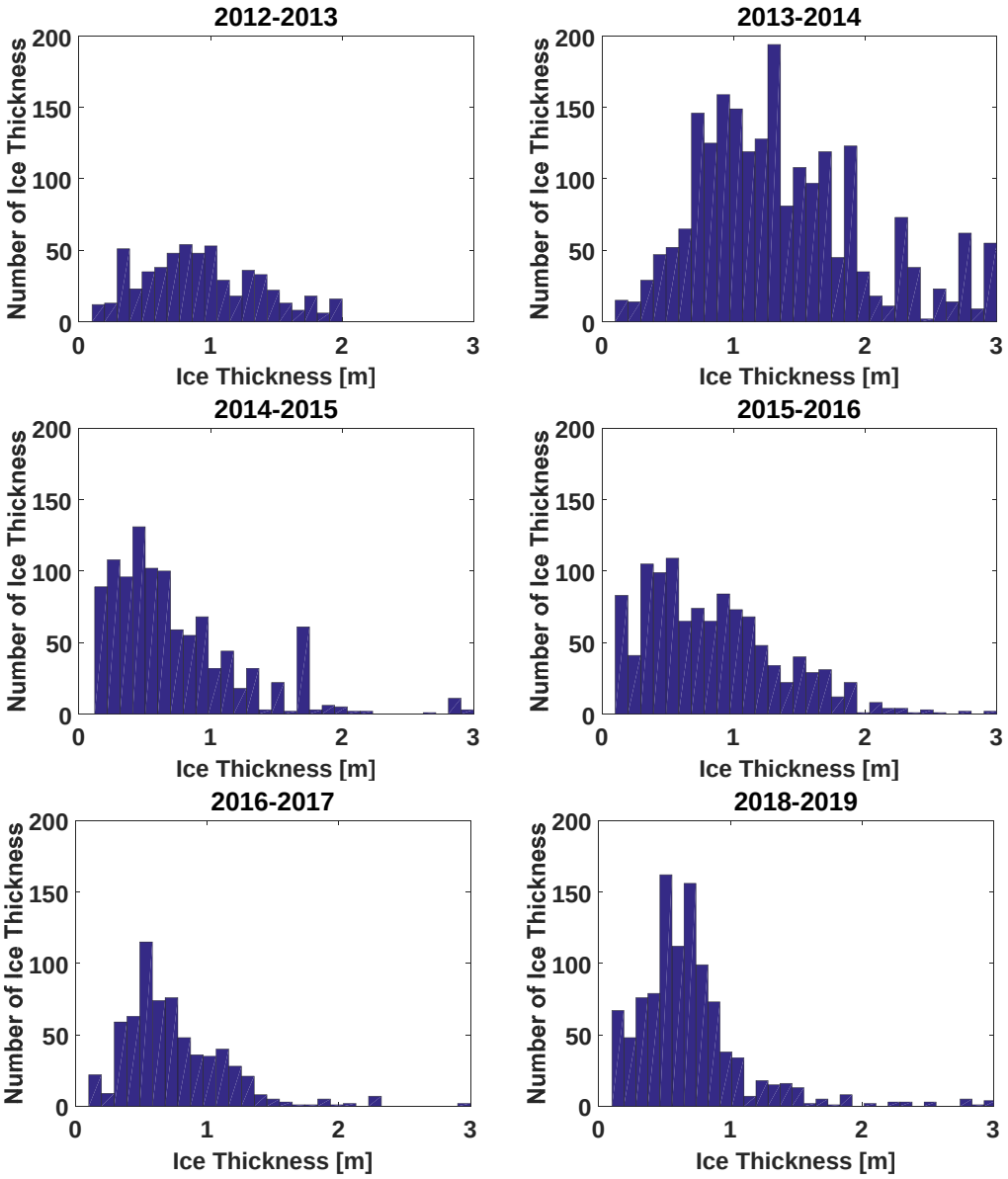

Figure 3. Ice thickness distribution

2.3 Local ice loads

The actual ice loads are continuous and recorded as time history curves. However, the hull is most possibly damaged by the extreme value of ice loads. Thus, this research focuses on the extreme value. The extreme ice loads are identified with two steps. Firstly, the Rayleigh separation is used to identify peak values of ice loads time history curve (Kujala et al, 2009). The second step is to select a maximum extreme load in a specific time interval. Consequently, the extreme ice loads are determined after the data processing.

Figure 4-6 show the distribution of ten minutes extreme loads on Frame #134+400, #112(1/2) and #40(1/2), respectively. These three frames typically represent the ice loads on the bow, bow shoulder and stern shoulder of the hull. The distribution figures reveal some common features of ice loads distribution on the three parts of hull. The first feature is that the number

of ice loads fluctuates with the variation of the number of ice thickness. For example, the largest number of ice thickness is observed in the summer between 2013 and 2014. The number of ice load is correspondingly the largest in this summer. The second feature is that although the numbers of ice loads decrease along with the increase of magnitude, the descending ratios are different year by year. Generally, the descending ratio is proportional to the total number of ice loads and the profile lines approximately converge at a specific ice load. The third feature is that the largest extreme ice load is not closely connected with the number of ice thickness. For example, the largest extreme load happed to Frame #134+400 from 2012 to 2013 is 1238 kN and the value from 2013 to 2014 is 1186 kN even though the numbers of ice thickness are 576 and 2158 in these two years, as shown in Table 2. Figure 4-6 also indicate that the magnitude and number of occurrence are much larger at bow than those of bow shoulder and stern shoulder. This means the situation at bow is the severest.

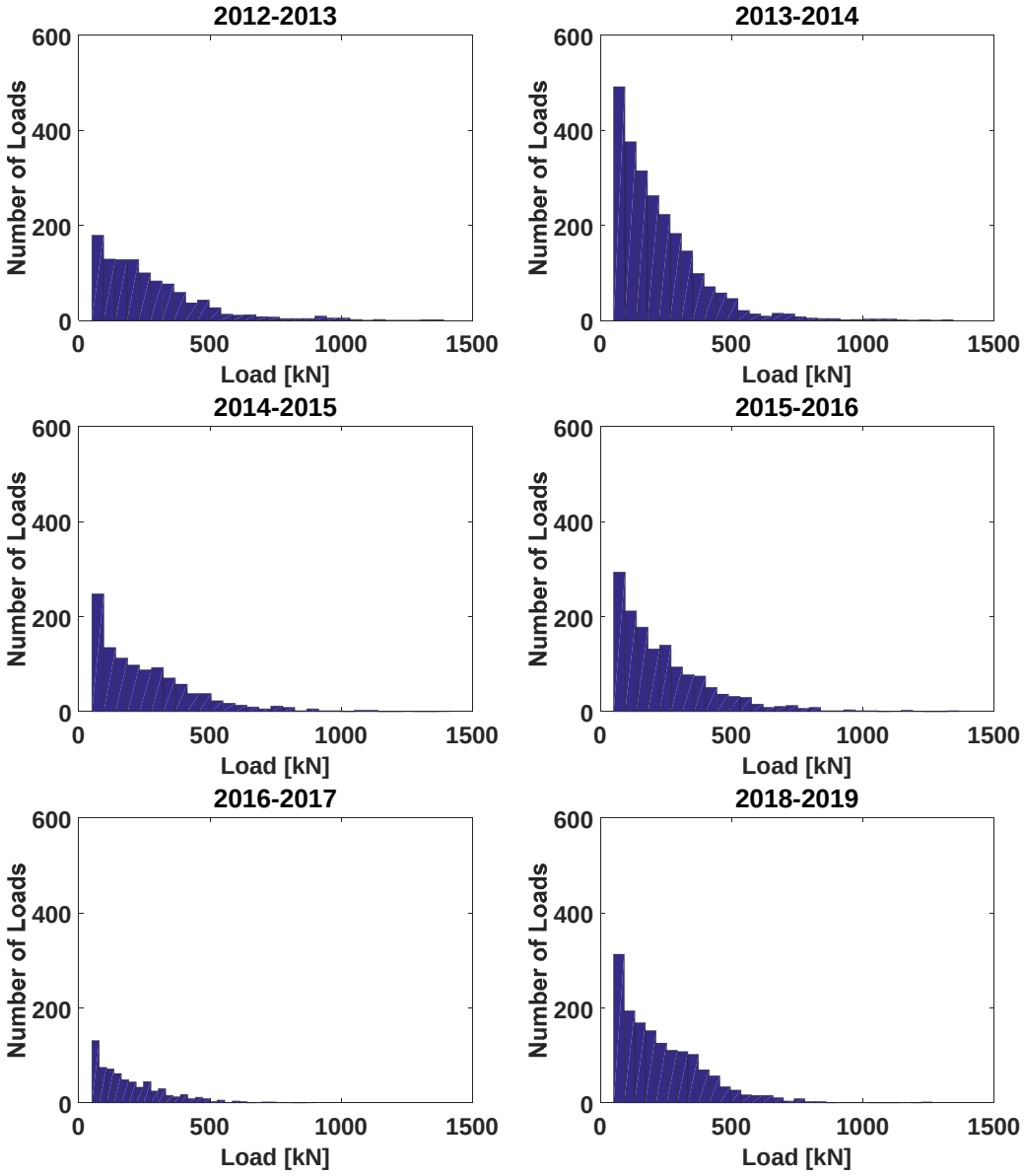

Figure 4. Ice loads distribution, Frame #134+400

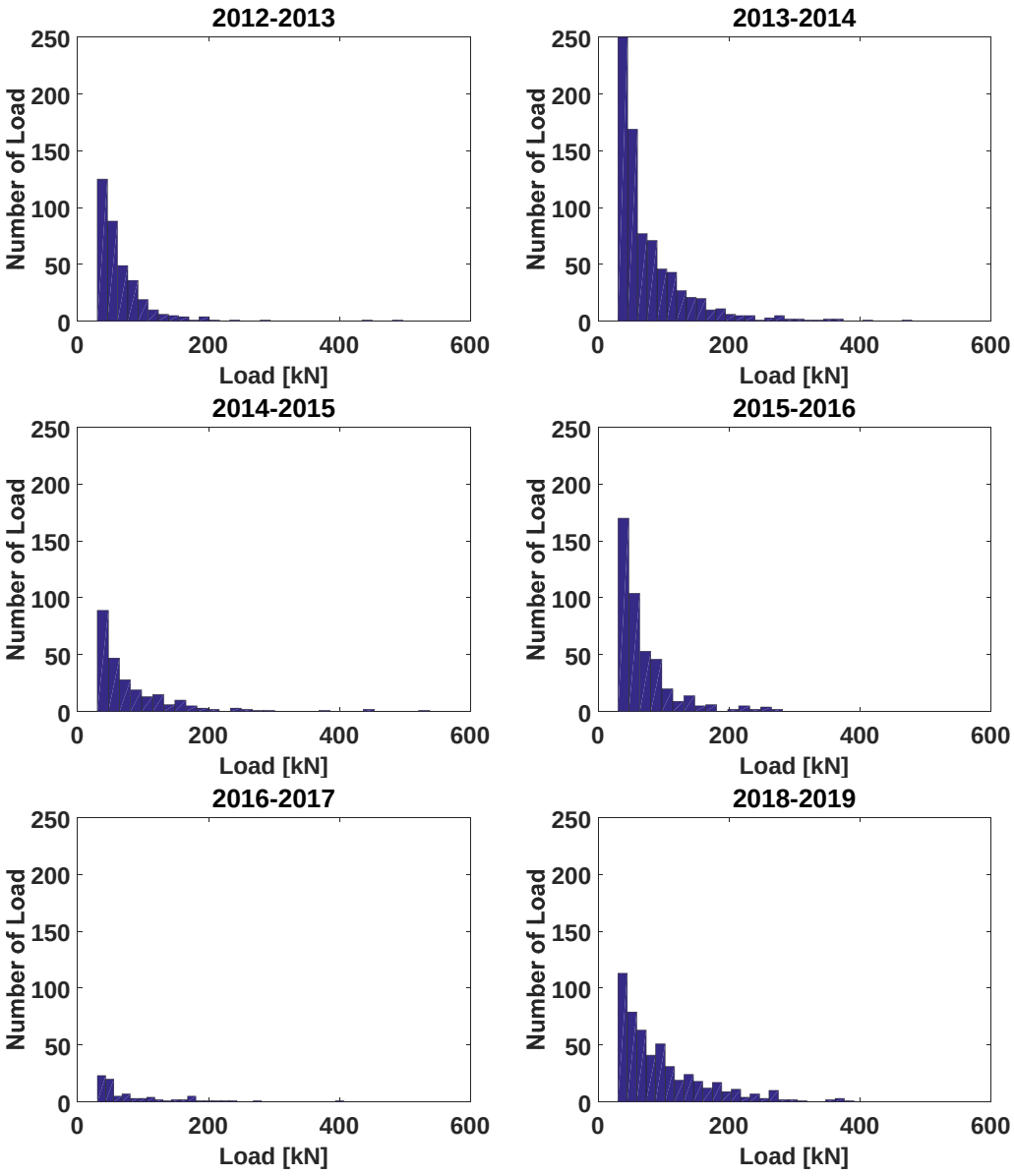

Figure 5. Ice loads distribution, Frame #112(1/2)

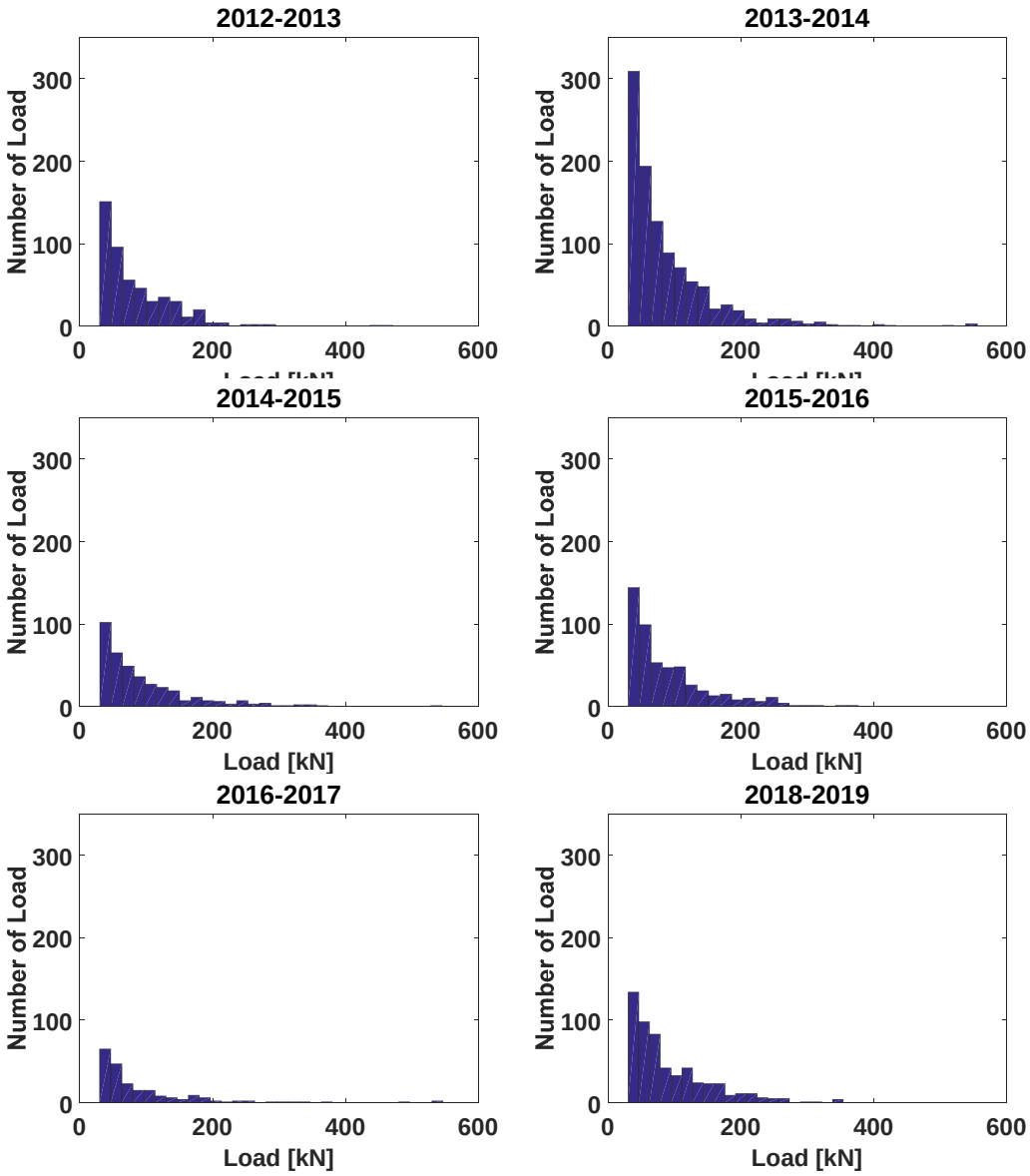

Figure 6. Ice loads distribution, Frame #40(1/2)

Figure 7 shows the return period of ice loads on Frame #134+400, #112(1/2) and #40(1/2) from 2012 to 2019. The number of ice load in 2018 is too small so it is not included in this analysis. This prediction uses annual measured 12 hours extreme data to predict the long term ice loads. The annual predictions obviously differs from each other, indicating the differences in the encountered ice conditions in different years. As discussed above, the ice loads are strongly influenced by the occurrence of ice contact, thus the ice loads prediction is influenced by the occurrence of ice contact as well. Therefore, it is understandable that different yearly ice conditions could lead to different ice loads predictions. However, the ice loads prediction is not related to the number of occurrence of ice loads. The largest numbers of ice loads on Frame #134+400, #112(1/2) and #40(1/2) were all recorded during the summer between 2013 and 2014. In contrast, the largest predictions of ice loads on Frame #134+400, #112(1/2) and #40(1/2) are derived from the measured data of 2012-2013, 2014-2015 and 2013-2014, respectively.

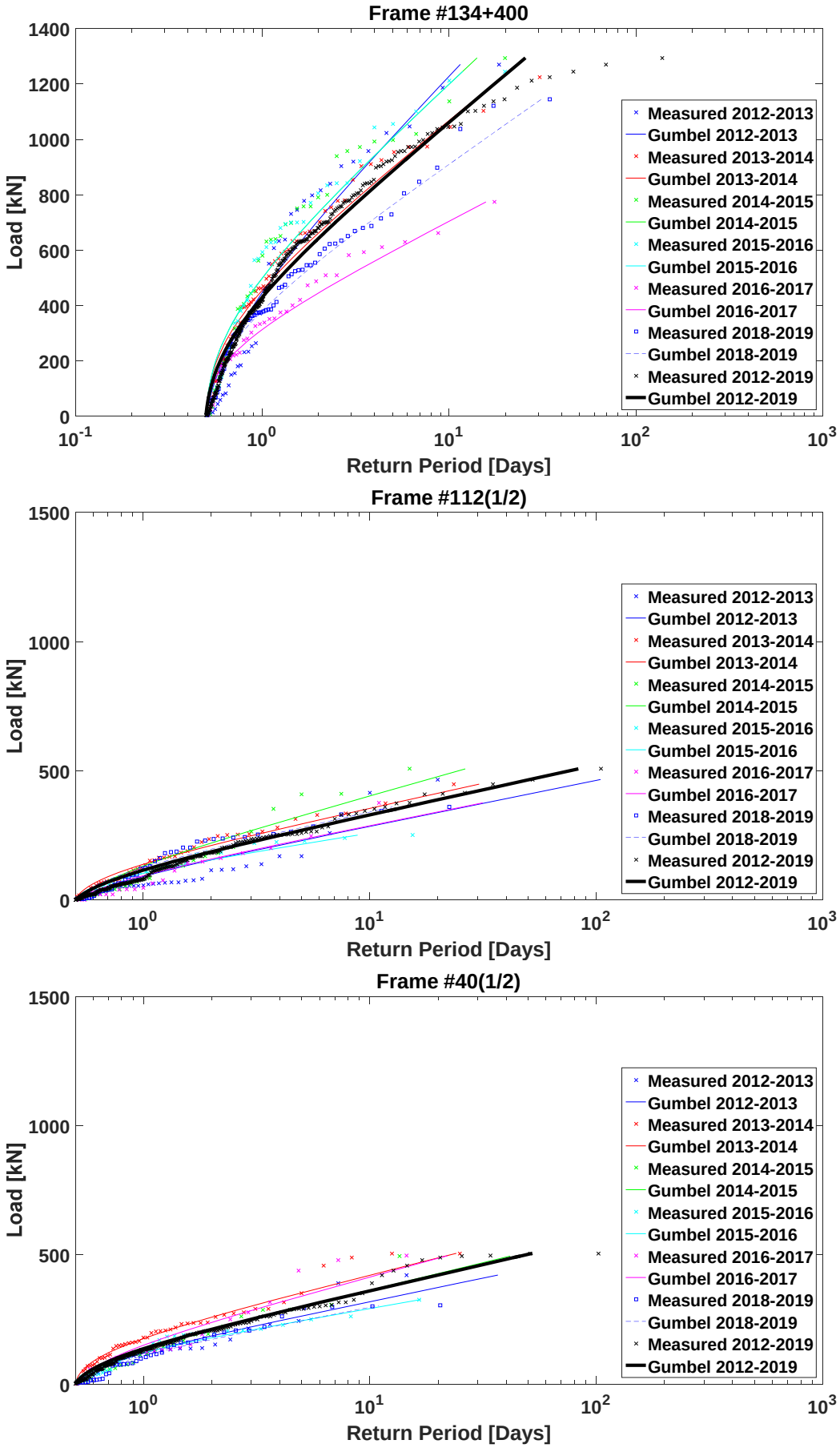

Figure 7. Return period of measured ice loads

3. Long term prediction based on Kujala's method

Kujala (1994) proposed a semi-empirical method to predict the long term ice load. This method includes the connection between ice loads and prevailing ice conditions. The mean ice thickness $\overline{h_l}$ and the standard deviation σ_i of ice thickness are obtained from the observation data base. The normal probability distribution is assumed to fit the probability density function of ice thickness

$$f(h_i) = \frac{1}{\sigma_i\sqrt{2\pi}} e^{-\frac{(h_i-\overline{h_l})^2}{2\sigma_i^2}} \tag{1}$$

In this method, the statistical mean of measured 12-hour extreme ice loads, m_{w_n}, is considered as piece-wise linearly related to the $\overline{h_l}$

$$\begin{cases} m_{w_n} = k_m^i \overline{h_l} & \overline{h_l} \le h_{max} \\ m_{w_n} = k_m^i h_{max} + k_m^a(\overline{h_l} - h_{max}) & \overline{h_l} \ge h_{max} \end{cases} \tag{2}$$

where k_m^i denotes the parameter for independent navigation in the level ice; k_m^a denotes the parameter for the navigation in broken ice field and h_{max} denotes the maximum ice breaking capability of the vessel. Figure 8 presents the mean ice loads and corresponding coefficient of variation induced by ice with specific thicknesses. The ice loads are separated into groups according to the ice thickness recorded by the observation, which increases from 0.1 m to 1.9 m with a step of 0.2 m. Each group's mean and standard deviation of ice loads are calculated for the calculation of k_m^i. The lines become horizontal after 1.0 m since k_m^a is assumed to be zero. The coefficient of variation, δ_{w_n}, is assumed to be independent of h_i

$$\delta_{w_n} = \frac{\sigma_{w_n}}{m_{w_n}} \tag{3}$$

where σ_{w_n} denotes the standard deviation of ice loads. Because m_{w_n} and σ_{w_n} are calculated from the measured ice loads on each frame, each frame has its own coefficients k_m^i, k_m^a and δ_{w_n}.

The extreme ice loads follow the Gumbel I asymptotic extreme value distribution so the cumulative distribution of extreme ice loads induced by the ice with a specific ice thickness can be calculated with

$$F_a\left(w_n/\overline{h_l}\right) = e^{-e^{-\frac{1}{c_n}(w_n-u_n)}} \tag{4}$$

where c_n and u_n are connected to the mean and coefficient of variation of the extreme ice loads

$$c_n = \frac{m_{w_n}\delta_{w_n}}{\pi/\sqrt{6}} \tag{5}$$

$$u_n = m_{w_n} - \gamma c_n \tag{6}$$

where $\gamma = 0.577$ denotes the Euler's constant. If the long term cumulative distribution function is extended to all thickness of ice, the normal distribution of ice thickness should be included

$$F(w_n) = \int_0^\infty F_a\left(w_n/\overline{h_l}\right) f(h_i)\, dh_i \tag{7}$$

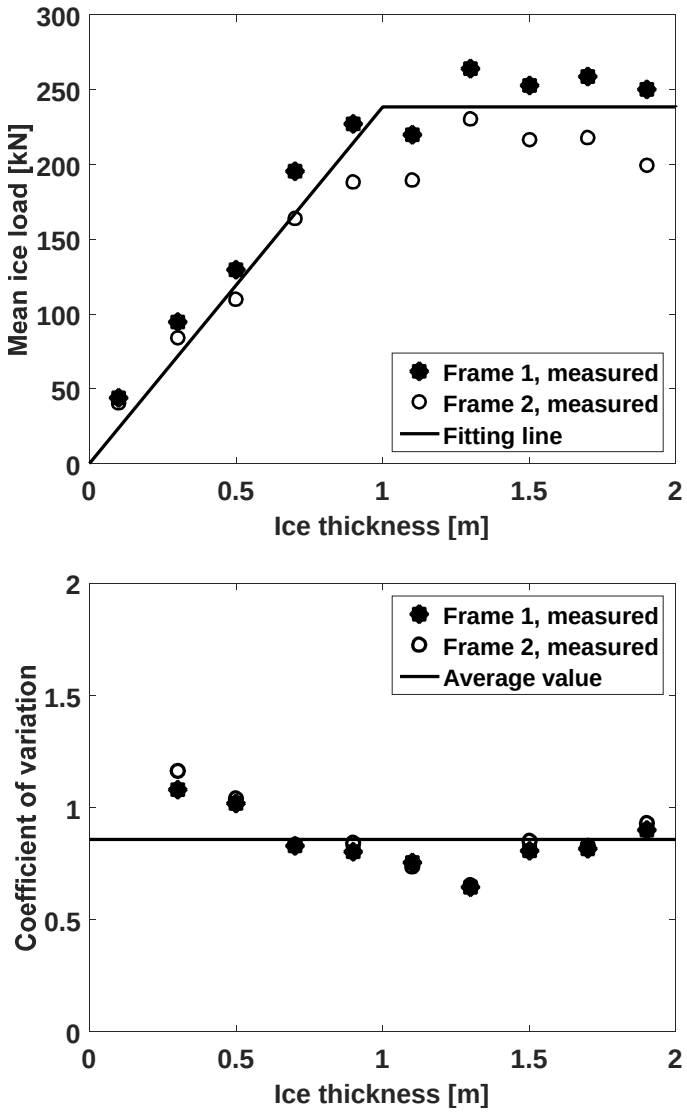

Figure 8. The relationship between the mean ice loads and ice thickness

Because the ice load data utilized here is 12 hour extreme ice loads, the time interval should be 0.5 days for the function of return period

$$T(w_n) = \frac{0.5}{1-F(w_n)} \tag{8}$$

Figure 9 shows the long term ice load prediction derived from Kujala's method and measured data from full scale measurement. Only Frame #134+400 and Frame #134 are presented as examples. The prediction and measured data are derived from five years data, from 2012 to 2019, because the previous discuss shows that the ice load can be strongly influenced by the ice condition and the ice condition varies year by year. Therefore, the data should be used as much as possible to provide more reliable prediction.

As the illustration, the prediction of Kujala's method fairly matches the measurement although the prediction for Frame #134+400 is larger at the highest part of the figure. The Gumbel I gives a better prediction when the return period is less than ten to thirty days. However, the Gumbel I predicts much higher load amplitude when the return period increases larger than ten days. Kujala's prediction matches the measurement better when the return period keeps rising although it also predicts higher load. More importantly, the results obtained here can be applied to predict ice loads on other ships by using Kujala's method.

The coefficients k_m^i and k_m^a can be applied for any other ice-strengthened ship in the sea around the Antarctic by considering the difference of frame angle (Kujala, 1994).

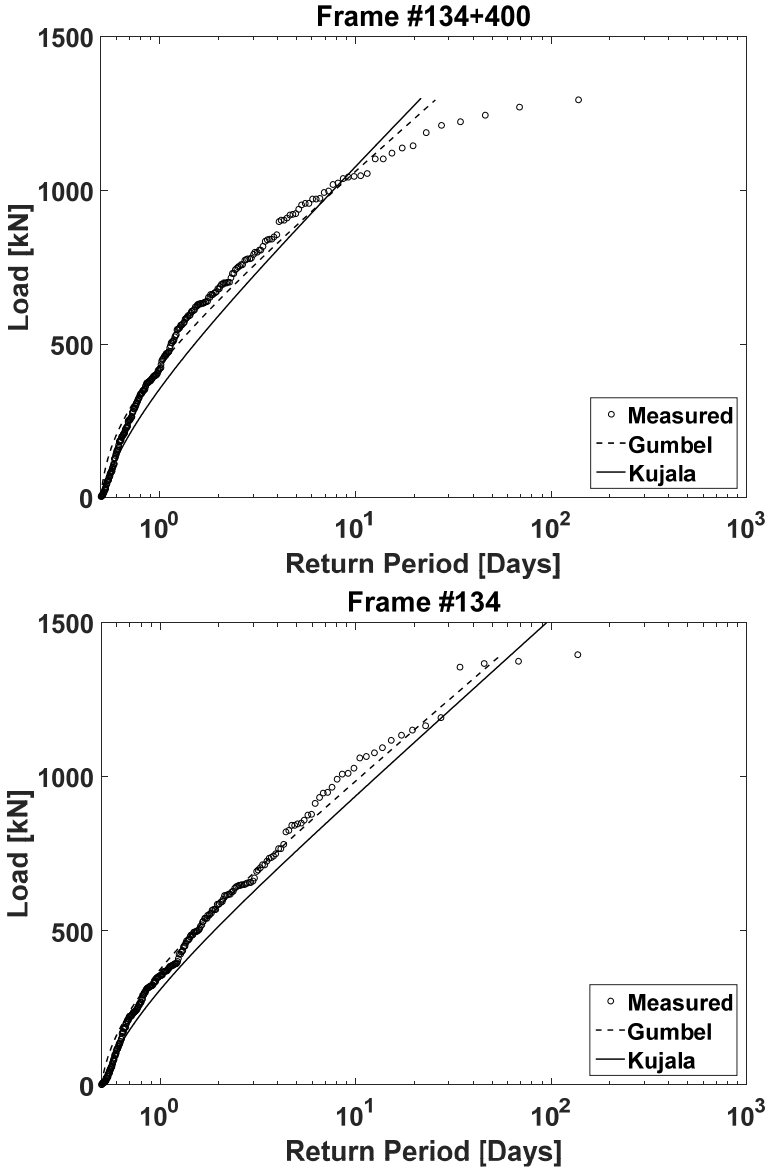

Figure 9. Return period of prediction and measurement

4. Conclusions

This paper firstly describe the full scale measurement of ice load and ice observation on board of S.A. Agulhas II. Then the ice thickness data recorded by visual observation are presented. After that, the record of ice loads is shown, which is measured on nine frames located at the bow, bow shoulder and stern shoulder. At last, Kujala's method is discussed for predicting long term ice load.

The record of visual observation shows that the ice conditions obviously vary year by year. The total number of observed ice thickness obviously fluctuates and the distribution of ice thickness also changes year by year. The variation of ice condition also induce the variation of ice loads from the magnitudes to the distribution. This causes the divergence of prediction of ice loads if annual data is used.

The method of Kujala (1996) can generate a fairly good long term prediction of ice loads. The Gumbel I distribution fits the measured data better when the return period is less than ten

days. Nevertheless, Kujala's method can provide a more precise prediction when the return period is larger than that. Furthermore, Kujala's method intends to employ the semi-empirical parameters achieving from the data measured on S.A. Agulhas II to predict the long term ice loads on another ships by a transformation based on the encountered ice conditions, the subjected ship's level ice breaking capability and frame angle. The validity of this method can be tested by comparing to possible measurement of other ships.

ACKNOWLEDGEMENT

This work is partly funded by SEDNA project, which has received funding from the European Research Council (ERC) under the European Union's Horizon 2020 research and innovation program (grant agreement n°723526). Funding from Lloyd Register Foundation are also gratefully acknowledged. The Lloyd's Register Foundation helps to protect life and property by supporting engineering-related education, public engagement and the application of research.

REFERENCES

Bekker, A., Suominen, M., Peltokorpi, O., Kulovesi, J., Kujala, P. and Karhunen J. 2014. Full-Scale Measurements on a Polar Supply and Research Vessel during Maneouver Tests in an Ice Field in the Baltic Sea. ASME 2014 33rd International Conference on Ocean, Offshore and Arctic Engineering, San Francisco, California, USA, June 8–13, 2014.

Chai, W., Leira, B.J. and Naess, A. 2018. Shor-term extreme ice loads prediction and fatigue damage evaluation for an icebreaker. Ships and Offshore Structures, vol.13, 127-137.

Kujala, P., 1989a. Probability based safety of ice-strengthened ship hull in the Baltic Sea. Licentiate Thesis. Helsinki University of Technology. Faculty of Mechanical Engineering. Espoo. 109 p. + app. 14p.

Kujala, P., 1989b. Results of long-term measurements on board chemical tanker Kemira in the Baltic Sea during the winters 1985 to 1988. Winter Navigation Research Board. Report 47. Helsinki. 55p + app. 137p.

Kujala P. 1994. On the statistics of ice loads on ship hull in the Baltic. PhD thesis, Acta polytechina scandinavica, mechanical engineering series No. 116. Helsinki, Finland. p. 98.

Kujala, P., 1996. Semi-empirical Evaluation of Long Term Ice Loads on a Ship Hull. Marine Structures, vol.9, 849-871.

Kujala, P., Goerlandt, F., Way, B., Smith, D., Yang, M., Khan, F. and Veitch, B. 2019. Review of risk-based design for ice-class ships. Marine Structures, Vol.63, 181-195.

Kujala, P., Suominen, M. and Riska, K. 2009. Statistics of ice loads measured on MT Uikku in the Baltic. Proceedings of the 20th International Conference on Port and Ocean Engineering under Arctic Conditions, Lulea, Sweden.

Suominen M, Aalto H, Kulovesi J, Lensu M, Kujala P, Soal K, Lehtiranta J. 2016. Ship-based ice thickness measurements in the Southern Ocean. 23nd IAHR international symposium on ice, Ann Arbor, Michigan USA, May 31 to June 3, 2016.

Suominen, M., Kujala, P., von Bock und Polach, R., and Kiviranta, J. 2013. Measured ice loads and design ice loads. The proceedings of the 4th Int. Conf. on Marine Structures (MARSTRUCT), Espoo, Finland, March 25-27, 2013.

Suominen, M., Kujala, P., Romanoff, J., & Remes, H. (2017). The effect of the extension of the instrumentation on the measured ice-induced load on a ship hull. Ocean Engineering, 144, 327-339.